# High spin states in $^{52}$Cr and $^{52}$Mn

P. Banerjee, B. Sethi, J. M. Chatterjee, M. B. Chatterjee, and P. Bhattacharya
*Saha Institute of Nuclear Physics, Bidhan Nagar, Calcutta 700 064, India*
(Received 7 April 1987)

High spin states in the two nuclei $^{52}$Cr and $^{52}$Mn, with $J^{\pi} \leq 11^{+}$, have been studied via the reactions $^{51}$V($\alpha$,p2n$\gamma$) and $^{51}$V($\alpha$,3n$\gamma$), respectively, by in-beam $\gamma$-ray spectroscopy. Measurements of lifetimes of excited states by the Doppler shift attenuation and recoil distance techniques, $\gamma$-ray angular distributions, excitation functions, and $\gamma\gamma$ coincidence, have been carried out in both the nuclei. New results obtained in $^{52}$Cr are the mean lifetime values of $0.35^{+0.25}_{-0.13}$, $0.23^{+0.22}_{-0.11}$, and $<2.0$ ps for the three highest observed states 8216.0 ($11^{+}$), 7237.1 ($10^{+}$), and 6453.4 keV ($9^{+}$), and multipole mixing ratios $-0.10^{+0.08}_{-0.05}$, $0.06^{+0.05}_{-0.03}$, and $-0.22^{+0.08}_{-0.15}$ for the 978.9, 784.7, and 629.1 keV $\gamma$ rays depopulating these states, respectively. In $^{52}$Mn, the lifetime of the 4163.4 keV ($10^{+}$) state, hitherto unreported, has been measured to be $0.20^{+0.35}_{-0.16}$ ps. Lifetimes of two other states in $^{52}$Mn, at 870.1 ($7^{+}$) and 2907.9 keV ($9^{+}$), for which only the upper limits were known previously, have been measured in this work and are found to be $0.07^{+0.08}_{-0.04}$ and $0.12\pm0.08$ ps, respectively. A comparison of the present experimental results on level lifetimes, multipole mixing ratios, and transition probabilities with the available theoretical calculations shows that most of the levels in $^{52}$Cr with excitation energies greater than 3.4 Mev are almost pure 1p5h states, while the lower lying states have a predominantly 0p4h configuration, with $\sim$20% 1p5h admixture. The observed $M1$ and $E2$ transition strengths between the high spin states in $^{52}$Mn favor interpretation of these states as having predominantly $(f_{7/2})^n$ configuration and provide evidence for the existence of collective features in this nucleus.

## I. INTRODUCTION

Studies of $fp$-shell nuclei at or near the neutron shell closure with $N=28$ is of special interest since these nuclei are ideal for description in the framework of the shell model. The excited states of these nuclei, including those with fairly large spins, have been interpreted in terms of pure shell model configurations.[1-3] The two nuclei $^{52}$Cr and $^{52}$Mn have been widely studied in this context[4-7] and many of the observed properties have been reasonably well explained in the light of the model calculations.

However, the experimental information regarding some of the high spin states, especially the highest observed ones in these two nuclei, is still inconclusive. For example, lifetime information in $^{52}$Cr is available only for states with excitation energy $E_x \leq 6.45$ MeV although levels up to $E_x = 8.22$ MeV and $J^{\pi} \leq (11^{+})$ have been experimentally observed.[8] The spin and parity assignments for the two energy levels at $E_x = 7.23$ and 8.22 MeV are ambiguous and the multipole mixing ratios for the $\gamma$ transitions depopulating these states are not known. Also, the existence of two close lying levels at $E_x \simeq 6.5$ MeV, first proposed by Berinde *et al.*,[9] is not established. In $^{52}$Mn, the studies of lifetimes of the high spin states with $J^{\pi} \leq (11^{+})$, reported by Avrigeanu *et al.*,[10] yielded only upper limit values, except for the 3.84 MeV state. As reported by the authors,[10] the uncertainty in their lifetime results arises mainly on account of a strong feeding of the high spin cascade in $^{52}$Mn by the $\beta^{+}$ decay of a $12^{+}$ isomer of $^{52}$Fe ($T_{1/2} = 56\pm8$ s). Considerable ambiguities therefore still remain regarding the electromagnetic properties and the spin and parity assignments for the high spin states in these two nuclei. The present investigation is aimed at resolving these ambiguities and permitting a more complete comparison of the experimental results with the available theoretical calculations.

## II. EXPERIMENTAL PROCEDURE

The present experiments have been carried out by in-beam $\gamma$-ray spectroscopy via the reactions $^{51}$V($\alpha$,p2n$\gamma$)$^{52}$Cr and $^{51}$V($\alpha$,3n$\gamma$)$^{52}$Mn using 30–45 MeV $\alpha$ particles, at the Variable Energy Cyclotron Centre, Calcutta. The lifetimes of the excited states in $^{52}$Cr and $^{52}$Mn have been measured using two Doppler-shift techniques, viz., the Doppler shift attenuation (DSA) and the recoil distance (RD) methods. Singles and a three parameter ($\gamma_1$-$\gamma_2$-t) measurements have been carried out to obtain the energy level scheme and to determine the placement of the $\gamma$ transitions. The spin assignments for some levels and the multipole mixing ratios of the depopulating $\gamma$ transitions have been determined by measurements of the $\gamma$-ray angular distributions. Excitation functions have been measured to supplement the results of angular distribution experiments.

Singles $\gamma$-ray spectroscopy was carried out using 40 MeV $\alpha$ particles, with beam currents typically in the range 2–5 nA. Self-supporting targets of natural vanadium ($^{51}$V, 99.8% abundant), 7.6 mg/cm$^2$ thick, were employed for the purpose. Two photon detectors were used for acquisition of the singles spectra. 25% Ge(Li) and 17% HPGe detectors were located at 90° and 125° to the beam direction, respectively, to obtain information on the $\gamma$-ray energies and their relative intensities.

 

The typical in-beam energy resolutions (FWHM) of the Ge(Li) and the HPGe detectors were found to be 2.7 and 2.4 keV, respectively, at 1333.6 keV ($^{52}$Cr). The data from the two detectors, recorded in two 4096 channel memories via two ADC's were periodically transferred to a magnetic tape from which they were analyzed subsequently. Standard efficiency calibrations for the two detectors were obtained using $^{60}$Co, $^{152}$Eu, and $^{207}$Bi sources under similar geometry. Precise energy information was obtained using internal lines in the spectra through a quadratic fit.

The three parameter ($\gamma_1$-$\gamma_2$-t) coincidence measurements were carried out with the two detectors placed 5 cm away from the target and perpendicular to the beam direction. Coincidence data were obtained in the list mode using conventional electronic set up and a Series 88 Canberra multichannel analyzer coupled to a magnetic tape unit. The data were subsequently analyzed in a Norsk Data (ND560) computer. Coincidence spectra for individual $\gamma$ rays were obtained by setting appropriate digital gates on the energy and time spectra (time window is 50 ns) subtracting the random events and those arising due to the Compton continuum of other $\gamma$ rays.

The excitation functions were studied at an angle of 125° to the beam direction, at projectile energies $E_\alpha = 30$, 35, 40, and 45 MeV. A large energy interval of 5 MeV between successive projectile energies was chosen since the excitation functions for the reactions of interest have large FWHM. The $\gamma$-ray yields measured at the four beam energies were normalized with respect to the integrated beam currents.

The angular distribution measurements were performed at four laboratory angles, namely 90°, 105°, 120°, and 140° at the projectile energy $E_\alpha = 40$ MeV, using a $\gamma$-X detector of 25% efficiency. The detector was placed at 20 cm from the target, and resulting solid angle corrections, being of the order of 5%, were neglected. The areas of the peaks of interest in the $\gamma$-ray spectra were normalized with respect to the areas of two prominent $\gamma$-ray lines, recorded simultaneously for the same time interval, in a monitor detector, placed at an angle of 125° to the beam direction. The angular distribution data were least squares fitted to the function $W(\theta) = A_0 + A_2 P_2(\cos\theta) + A_4 P_4(\cos\theta)$. The spin alignment attenuation coefficients $\alpha_2(J) = A_2 / A_2^{\max}$, required for a quantitative analysis of the angular distribution data have been calculated for different $J$ values, following the method of Ejiri *et al.*[11]. The corresponding $\alpha_4(J)$ values were taken from Ref. 12. The calculated $\alpha_2(J)$ values show fair agreement with the experimentally determined ones for the levels depopulating via pure $E2$ transitions. These $\alpha_k(J)$ values were used to obtain the theoretical angular distributions. For each transition, a $\chi^2(\delta)$ analysis was carried out to determine the spin assignments and multipole mixing ratio ($\delta$)

The Doppler shift attenuation measurements for the study of lifetimes in $^{52}$Cr and $^{52}$Mn were carried out via the same reactions as mentioned earlier at $E_\alpha = 40$ MeV. The energetic recoiling nuclei were stopped in the thick target itself, whose thickness (7.6 mg/cm$^2$) was sufficient to stop ~95% of the recoiling nuclei and allow the beam to pass through to the beam dump. The experimental attenuation factors, $F(\tau)_{\text{exp}}$ were obtained from the centroid shift measurements of the Doppler broadened lines recorded at $\theta_\gamma = 55°$, 105°, 120°, and 140° with respect to the corresponding centroids at $\theta_\gamma = 90°$. The method of estimation of the lifetime from the experimental $F(\tau)$ values is described elsewhere.[13,14] The corrections to the lifetime values on account of sidefeeding have been applied following the procedure outlined in Ref. 23, assuming that the sidefeeding times are $\leq$ 0.1 ps for both $^{52}$Cr and $^{52}$Mn. An evidence supporting this assumption is found in the present work in the case of $^{52}$Mn where the attenuation factor $F(\tau)$ for the 870.1 keV $\gamma$ ray ($7^+ \rightarrow 6^+$ transition), corrected only for the effects of the observed cascade feedings, corresponds to an apparent meanlife $\tau \sim 0.1$ ps.

Lifetimes in the picosecond range have been measured by the recoil distance method using an experimental set up similar to the one described by Alexander and Bell.[15] Target thicknesses, typically 100–150 $\mu$g/cm$^2$, were used for these experiments. A thin stretched stopper, of thickness just sufficient to stop the recoiling nuclei emerging from the target, was used in order to reduce the level of background $\gamma$ radiations usually associated with a conventional thick stopper. The target stopper separation was monitored by an rf technique described in Ref. 16.

## III. EXPERIMENTAL RESULTS

The experimental results for the two nuclei $^{52}$Cr and $^{52}$Mn are presented in the following.

### A. The nucleus $^{52}$Cr

A typical singles $\gamma$-ray spectrum, recorded at 90° to the beam direction, is shown in Fig. 1. Prominent $\gamma$-ray lines belonging to $^{52}$Cr are indicated in the figure. The $\gamma$-ray energies and their relative intensities are given in Table I along with the earlier results.[8,9,17] A comparison of the relative intensities shows that the high spin yrast states in $^{52}$Cr are more strongly populated in the present work in comparison with the reactions $^{50}$Ti($\alpha$,2n$\gamma$) and $^{51}$V($^{6,7}$Li,$\alpha x$n$\gamma$), reported earlier.

The level scheme for $^{52}$Cr determined in this work is shown in Fig. 2. The present work confirms the seven high spin states at 4805.9, 5397.2, 5824.3, 6452.4, 6453.4, 7237.1, and 8216.0 keV. While the first six levels were first reported by Berinde *et al.*,[9] the level at 8216.0 keV has been reported by Styczen *et al.*[8] only. Many of the low spin states reported previously[18] have not been observed via the reaction $^{51}$V($\alpha$,p2n$\gamma$).

The placement of the $\gamma$ transitions is based mainly on the coincidence relationships obtained from the three parameter measurements. Typical gated energy spectra with energy windows at 427.1, 629.1, 744.8, and 1434.0 keV are shown in Fig. 3. Contrary to the results of Berinde *et al.*,[9] the 629.1 keV transition is not found to be a doublet. Its assignment in the level scheme is based on the observation of this line in coincidence with the 427.1

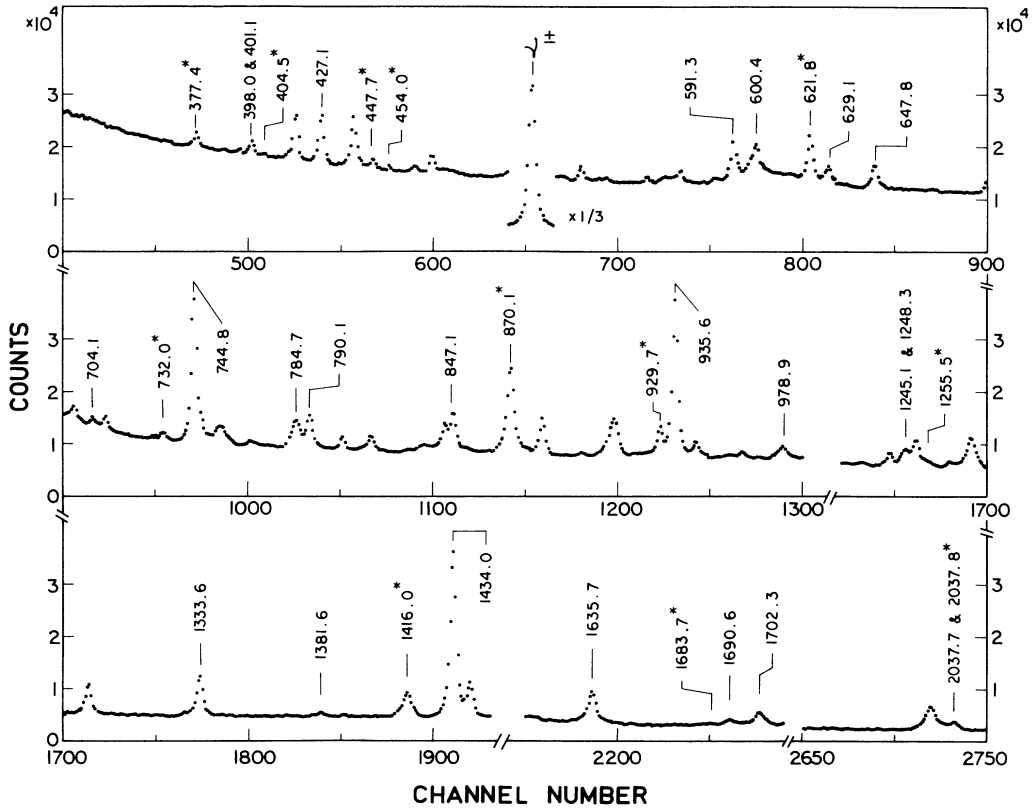


FIG. 1. Singles $\gamma$-ray spectrum obtained from the bombardment of natural vanadium target with 40 MeV $\alpha$ particles, recorded at 90° to the beam direction. Only the $\gamma$-ray lines belonging to $^{52}$Cr and $^{52}$Mn, the latter marked with asterisks, are labeled. The alpha energies are given in keV.

TABLE I. Energies and relative intensities of $\gamma$ rays depopulating the yrast states in $^{52}$Cr, measured at 90° and 125°, respectively, to the beam direction, in the reaction $^{51}$V($\alpha$,p2n$\gamma$) at $E_\alpha = 40$ MeV. These states are better populated in this reaction compared to the reactions $^{50}$Ti($\alpha$,2n$\gamma$) (Refs. 8 and 9) and $^{51}$V($^7$Li,$\alpha$2n$\gamma$), $^{51}$V($^6$Li,$\alpha$n$\gamma$) (Ref. 17).

| Level energy $E_x$ (keV) | $E_\gamma$ (keV) $J_i^\pi \rightarrow J_f^\pi$ | Relative $\gamma$-ray intensity $I_\gamma$ Present work | Ref. 8 | Previous Ref. 9 | Ref. 17 |
|---|---|---|---|---|---|
| 1434.0 | 1434.0 $2^+ \rightarrow 0^+$ | 100±5.0 | 100 | 100±5.1 | 100 |
| 2369.6 | 935.6 $4^+ \rightarrow 2^+$ | 61.7±3.1 | 58.8±3.2 | 57.3±2.0 | 30.0±0.4 |
| 3114.4 | 744.8 $6^+ \rightarrow 4^+$ | 51.1±2.6 | 36.2±2.0 | 39.7±1.2 | 22.1±0.2 |
| 4750.1 | 1635.7 $8^+ \rightarrow 6^+$ | 33.0±1.7 | 22.3±1.2 | 12.2±0.5 | 7.2±0.6 |
| 6452.4 | 1702.3 $9^+ \rightarrow 8^+$ | 8.8±0.5 | 7.7±0.4 | 8.7±0.6 | |
| 7237.1 | 784.7 $10^+ \rightarrow 9^+$ | 8.7±0.4 | 4.2±0.5 | 1.7±0.6 | |
| 8216.0 | 978.9 $11^+ \rightarrow 10^+$ | 5.8±0.3 | 2.1±0.2 | | |

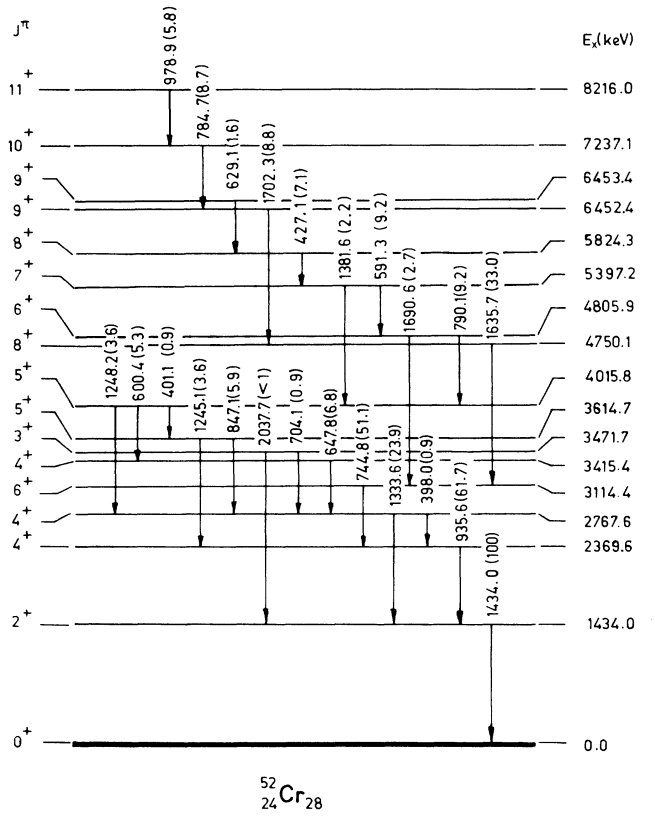


FIG. 2. Level scheme of $^{52}$Cr showing $\gamma$-ray transitions obtained in the present work. The relative $\gamma$-ray intensities measured at 125°, in the reaction $^{51}$V($\alpha$,p2n$\gamma$) at $E_\alpha = 40$ MeV, are given in parentheses. The estimated errors in the intensities are 5% for relative intensity values in the range 5–100 and 5–15 % for weaker $\gamma$ rays.

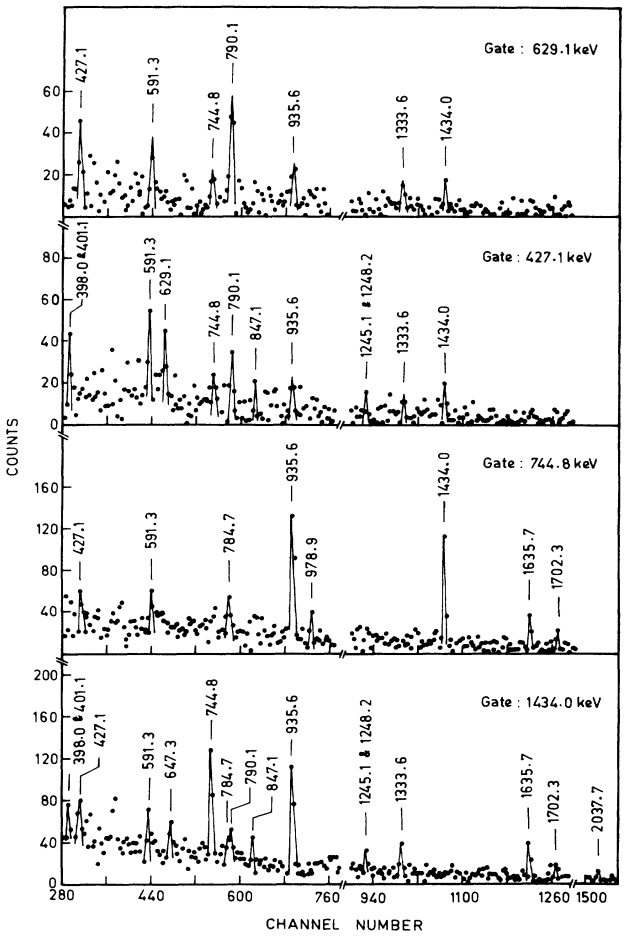


FIG. 3. Gated $\gamma$-ray energy spectra for $^{52}$Cr with energy windows at 629.1, 427.1, 744.8, and 1434.0 keV. Conversion gain for the spectra is 1.33 keV/channel. The superimposed peaks are shown only to indicate the position of the $\gamma$-ray lines in the spectra.

keV transition and is shown to depopulate the level at 6453.4 keV. However, as proposed by Berinde *et al.*,[9] the present work supports the possibility of the existence of two close lying levels at 6452.4 and 6453.4 keV. This result is based on the fact that the 784.7 keV transition is observed in coincidence with the 744.8, 935.6, 1434.0, 1635.7, and 1702.3 keV transitions while it is not seen in coincidence with the 427.1 and 629.1 keV $\gamma$ rays. The inference drawn from the coincidence with the 784.7 keV gate is not unambiguous due to the presence of the close-lying 790.1 keV $\gamma$ ray, which is coincident with the 629.1 keV transition. It is nevertheless reasonable to conclude that the 629.1 keV transition does not depopulate the same level which the 784.7 keV $\gamma$-ray feeds and hence the conclusion that there are two separate levels. This, however, is in contradiction with the result reported by Styczen *et al.*[8] The placement of the 784.7 and 978.9 keV $\gamma$ transitions depopulating the levels at 7237.1 and 8216.0 keV is consistent with the earlier results.[8,9]

The placement of the 2037.7 keV transition, tentatively assigned previously,[9] is ascertained from the coincidence with the 1434.0 keV energy gate to connect the levels at 3471.7 and 1434.0 keV. This argument is supported by the fact that the 2037.7 keV transition is not seen in coincidence with any of the other energy windows.

Angular distribution measurements were carried out for ten $\gamma$-ray transitions in $^{52}$Cr, viz., 427.1., 629.1, 744.8, 784.7, 935.6, 978.9, 1333.6, 1434.0, 1635.7, and 1702.3 keV. The angular distributions for the four $\gamma$-ray transitions depopulating the four highest observed levels are shown in Fig. 4. The values of the coefficients $(A_2/A_0)_{\text{exp}}$ and $(A_4/A_0)_{\text{exp}}$ for each transition are given in Table II. The spin value ($J$) for the levels and the multipole mixing ratio ($\delta$) for the $\gamma$-rays depopulating the levels are determined from a $\chi^2$ analysis taking three probable spin sequences for each transition. The $\chi^2(\delta)$ vs $\delta$ plot for the 784.7 keV transition depopulating the 7237.1 keV level is shown in Fig. 5. The adopted spin sequences and the values of the mixing ratio $\delta$ corresponding to the minimum minimorum in $\chi^2(\delta)$ are also given in Table II.

The $J$ values for the 6453.4, 7237.1, and 8216.0 keV levels have been determined conclusively in the present work. Taking the spin value $J=7$ for the 5397.2 keV state,[9] the spin values for the 5824.3 and 6453.1 keV levels are determined to be $J=8$ and 9, respectively, based

TABLE II. Results of angular distribution measurements in $^{52}$Cr.

| Level energy $E_x$ (keV) | $\gamma$-ray energy $E_\gamma$ (keV) | Angular distribution coefficients $(A_2/A_0)_{exp}$ | $(A_4/A_0)_{exp}$ | Adopted spin sequence $J_i \rightarrow J_f$ | Multipolarity mixing ratio $\delta$ |
|---|---|---|---|---|---|
| 1434.0 | 1434.0 | 0.24±0.04 | −0.12±0.05 | $2\rightarrow 0$ | $E2$ |
| 2369.6 | 935.6 | 0.31±0.09 | −0.08±0.10 | $4_1\rightarrow 2$ | $E2$ |
| 2767.6 | 1333.6 | 0.27±0.06 | −0.05±0.07 | $4_2\rightarrow 2$ | $E2$ |
| 3114.4 | 744.8 | 0.30±0.05 | −0.13±0.05 | $6_1\rightarrow 4_1$ | $E2$ |
| 4750.1 | 1635.7 | 0.32±0.07 | −0.09±0.08 | $8_1\rightarrow 6_1$ | $E2$ |
| 5824.3 | 427.1 | −0.26±0.09 | −0.12±0.11 | $8_2\rightarrow 7$ | 0.03±0.04 |
| 6452.4 | 1702.3 | −0.20±0.09 | 0.02±0.12 | $9_1\rightarrow 8_1$ | $0.04^{+0.03}_{-0.07}$ |
| 6453.4 | 629.1 | −0.67±0.21 | −0.03±0.26 | $9_2\rightarrow 8_2$ | $-0.22^{+0.08}_{-0.15}$ |
| 7237.1 | 784.7 | −0.13±0.07 | −0.02±0.08 | $10_1\rightarrow 9_1$ | $0.06^{+0.05}_{-0.03}$ |
| 8216.0 | 978.9 | −0.27±0.15 | 0.18±0.19 | $11_1\rightarrow 10_1$ | $-0.10^{+0.08}_{-0.05}$ |

on angular distribution measurements on the 427.1 and 629.1 keV $\gamma$ rays. The angular distribution for the 784.7 keV transition has been performed for the first time and establishes the spin value for the 7237.1 keV state to be $J=10$. The $J$ value for the 8216.0 keV state, tentatively assigned to be 11 by Styczen *et al.*,[8] is confirmed in the present work, based on the angular distribution measurements on the 978.9 keV $\gamma$ ray. The present work also confirms the spin assignment $J=9$ for the 6452.4 keV state which decays via the 1702.3 keV $\gamma$ ray. The spin assignments for the lower lying states with excitation energy $E_x \leq 4750.1$ keV (Table II) depopulating by strong $E2$ transitions, determined from the present angular distribution and excitation function measurements are consistent with previous reports.[18]

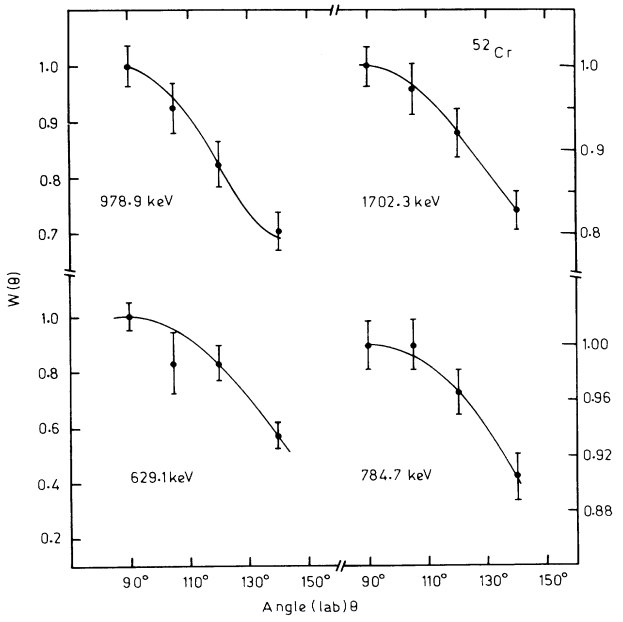


FIG. 4. Angular distributions and least squares fits to the function $W(\theta)=A_0+A_2P_2(\cos\theta)+A_4P_4(\cos\theta)$ for the $\gamma$-ray transitions depopulating the four highest observed states in $^{52}$Cr.

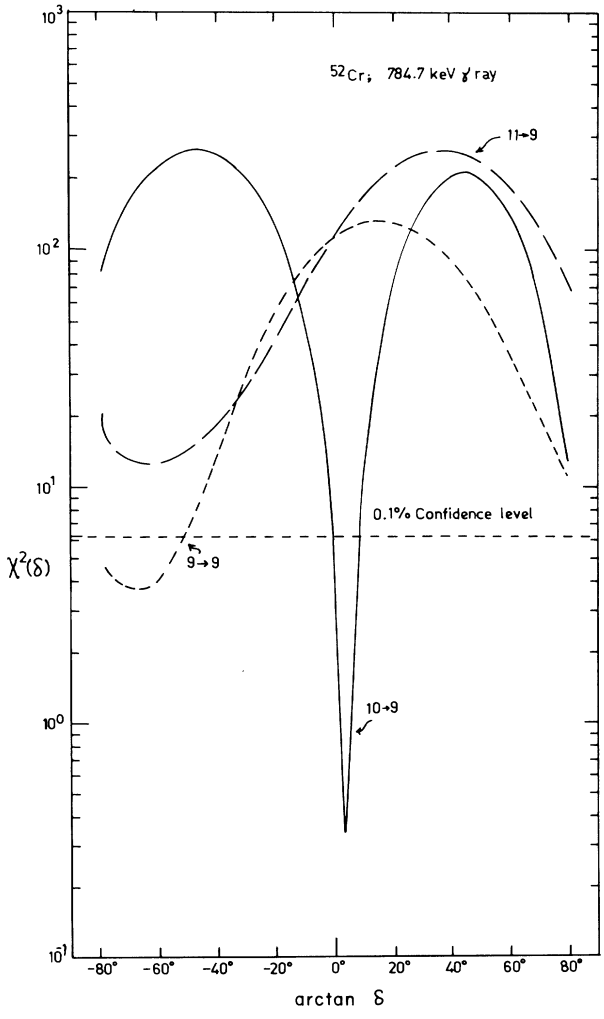


FIG. 5. The least-squares $\chi^2$ fits versus arctan $\delta$ to the angular distribution of the 784.7 keV transition depopulating the 7237.1 keV state in $^{52}$Cr for the indicated spin sequences $(J_i \rightarrow J_f)$.

The multipolarities and the mixing ratios for the 978.9, 784.7, and 629.1 keV transitions depopulating the 8216.0, 7237.1, and 6453.4 keV states, respectively, have not been previously reported in the literature. The analyses of the angular distributions lead to prodominantly dipole assignments for the 978.9 and 784.7 keV transitions and a 5% quadrupole admixture for the 629.1 keV transition. The 427.1 keV transition ($\delta=0.03\pm0.04$) from the 5824.3 keV state is found to be almost pure dipole in character in agreement with the results of Styczen *et al.*[8] but in serious disagreement with that of Berinde *et al.*[9] who reported $\delta=-9.51^{+3.43}_{-11.96}$ for this transition.

The mean lifetimes of seven levels at 3415.4, 4750.1, 4805.9, 5824.3, 6452.4, 7237.1, and 8216.0 keV have been measured by the DSA and for the 3114.4 keV level by the recoil distance method. Also, upper limits of lifetime values have been obtained for the two levels at 4015.8 and 6453.4 keV. The results of lifetime measurements and deduced $B(E2)$ and $B(M1)$ values are given in Table III. Typical Doppler broadened line shapes obtained at $\theta_\gamma=140°$ for a few transitions are shown in Fig. 6. The lifetime information for the 6453.4, 7237.1, and 8216.0 keV levels is being reported for the first time.

The DSA measurements for the 647.8 keV $\gamma$ ray yield an apparent mean life of $\tau=0.85^{+0.40}_{-0.20}$ for the 3415.4 keV level. However, corrections due to the strong cascade feeding from the relatively long lived 4015.8 keV level, combined with the effects of direct feeding, lead to a mean life $\tau=0.15^{+0.11}_{-0.08}$ ps. The significant disagreement of the result with the value reported by Berinde *et al.*[9] (0.63±0.14 ps) is understandable, since the latter result as mentioned by the authors is uncorrected for the cascade feeding effects. Presumably, the present result also disagrees with the mean of the two other previous results[17,19] due to similar reasons.

An upper limit of mean life $\tau<1.7$ ps is obtained for the 4015.8 keV level on the basis of the observation of a small Doppler shift [$F(\tau)=0.13$]. The lifetime of the 4805.9 keV level is found to be $\tau=0.70^{+0.40}_{-0.20}$ ps. The direct feedings to these levels are found to be small ($<10\%$) and account for the fair agreement of the present lifetime results for these two states with the values reported by Berinde *et al.*[9] As pointed out by the authors,[9] their lifetime results represent upper limit values. This is due, possibly on account of the fact that corrections due to direct feedings were not included in their work. Since the direct feedings to most of the other levels (discussed below) are significant, the present lifetime results, corrected for the effects of both cascade and direct feedings, for these states, are found to be consistently smaller compared to the results reported in Ref. 9.

Lifetime of the 3114.4 keV state, measured by the recoil distance method in the present work, agrees closely with the value reported in Ref. 17 but differs widely

TABLE III. Results of lifetimes and reduced transition probabilities in $^{52}$Cr.

| $E_x$ (keV) | $E_\gamma$ (keV) $J_i^\pi\rightarrow J_f^\pi$ | Mixing ratio $\delta$ | Mean lifetimes $\tau$ (ps) Present | Previous | Reduced transition strengths (W.u.) $E2$ | $M1$ |
|---|---|---|---|---|---|---|
| 3114.4 | 744.8 $6_1^+\rightarrow4_1^+$ | $E2$ | $65.2\pm8.1$ | $3.61^{+1.14}_{-0.95}$ [a]<br>$60\pm2.6$ [b] | $4.76^{+0.68}_{-0.53}$ | |
| 3415.4 | 647.8 $4_3^+\rightarrow4_2^+$ | $0.16\pm0.11$ [d] | $0.15^{+0.11}_{-0.08}$ | $0.63\pm0.14$ [a]<br>$0.48\pm0.12$ [b]<br>$0.32^{+0.12}_{-0.07}$ [c] | $104^{+501}_{-97}$ | $0.76^{+0.89}_{-0.35}$ |
| 4015.8 | 600.4 $5_2^+\rightarrow4_3^+$ | | $<1.7$ | $1.00\pm0.74$ [a]<br>$0.84^{+0.46}_{-0.28}$ [c] | | |
| 4750.1 | 1635.7 $8_1^+\rightarrow6_1^+$ | $E2$ | $0.43^{+0.25}_{-0.17}$ | $0.93^{+0.29}_{-0.25}$ [a]<br>$<6$ [b] | $14.13^{+9.23}_{-5.20}$ | |
| 4805.9 | 790.1 $6_2^+\rightarrow5_2^+$ | $0.16\pm0.05$ [e] | $0.70^{+0.40}_{-0.20}$ | $0.78^{+1.73}_{-0.47}$ [a] | $6.34^{+8.68}_{-4.41}$ | $0.07\pm0.03$ |
| 5824.3 | 427.1 $8_2^+\rightarrow7^+$ | $0.03\pm0.04$ | $0.42^{+0.24}_{-0.14}$ | $1.5^{+0.91}_{-0.55}$ [a] | $10.71^{+76.44}_{-9.95}$ | $0.97^{+0.47}_{-0.36}$ |
| 6452.4 | 1702.3 $9_1^+\rightarrow8_1^+$ | $0.04^{+0.03}_{-0.07}$ | $0.20^{+0.18}_{-0.12}$ | $0.42^{+0.18}_{-0.15}$ | $0.04^{+0.26}_{-0.03}$ | $0.03^{+0.05}_{-0.01}$ |
| 6453.4 | 629.1 $9_2^+\rightarrow8_2^+$ | $-0.22^{+0.08}_{-0.15}$ | $<2.0$ | | $>7$ | $>0.06$ |
| 7237.1 | 784.7 $10_1^+\rightarrow9_1^+$ | $0.06^{+0.05}_{-0.03}$ | $0.23^{+0.22}_{-0.11}$ | | $3.73^{+20.09}_{-3.25}$ | $0.28^{+0.27}_{-0.14}$ |
| 8216.0 | 978.9 $11^+\rightarrow10^+$ | $-0.10^{+0.08}_{-0.05}$ | $0.35^{+0.25}_{-0.13}$ | | $2.24^{+5.67}_{-2.19}$ | $0.10^{+0.05}_{-0.06}$ |

[a]Reference 9.
[b]Reference 17.
[c]Reference 19.
[d]Mean of $\delta$ values reported in Ref. 8 and Ref. 22.
[e]Reference 8.

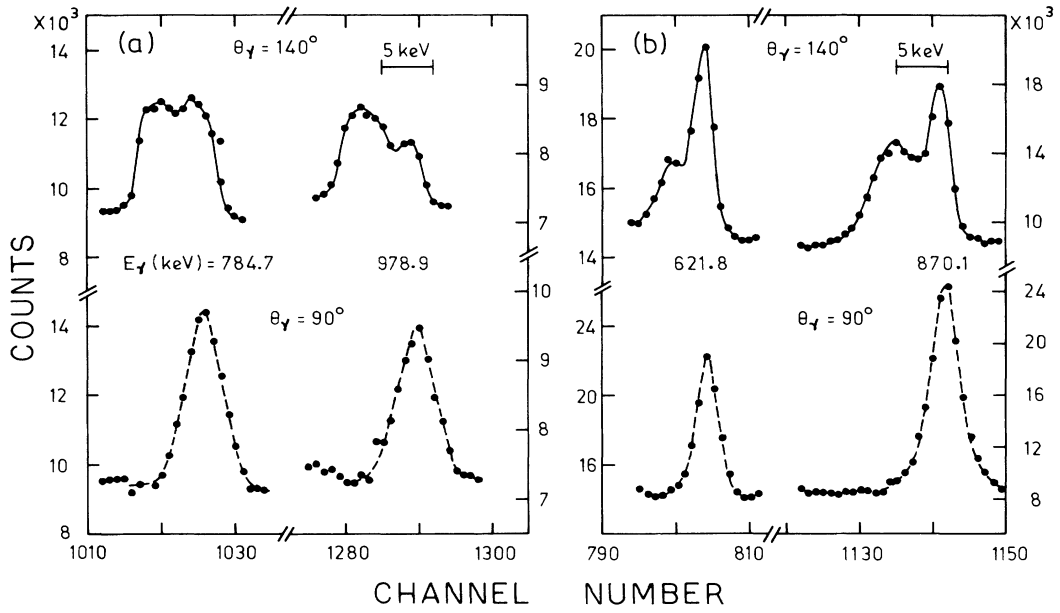


FIG. 6. Typical Doppler-broadened peaks (continuous lines) observed at $\theta_\gamma = 140°$ and the corresponding unshifted peaks (broken lines) at 90° to the beam direction for (a) the 784.7 and 978.9 keV $\gamma$ rays of $^{52}$Cr, and (b) the 621.8 and 870.1 keV $\gamma$ rays of $^{52}$Mn.

with the DSA result of Berinde *et al.*[9] The $B(E2)$ and $B(M1)$ values for the 744.8, 647.8, and 790.1 keV transitions, deduced from the present lifetime results for the 3114.4, 3415.4, and 4805.9 keV states, are consistent with the earlier parity assignments for these states (Table III).

The results for the high spin states ($J \geq 8$) observed in the present work are discussed in the following.

*The 4750.1 keV level.* The DSA analysis of the 1635.7 keV $\gamma$-ray depopulating the 4750.1 keV level yields a mean life $\tau = 0.43^{+0.25}_{-0.17}$ ps, which agrees within errors with the earlier result.[9] The meanlife value, uncorrected for the effects of direct feeding, is $0.56^{+0.31}_{-0.18}$ ps. As seen from the angular distribution results, the 1635.7 keV $\gamma$ ray is a $8^+ \rightarrow 6^+$, $E2$ transition. The value of the reduced transition probability $B(E2) = 14.1^{+9.2}_{-5.2}$ W.u. supports the assignment of the positive parity to the 4750.1 keV state.

*The 5824.3 keV level.* The level deexcites via the 427.1 keV $\gamma$ transition which is found to be predominantly $M1$ from the present angular distribution measurements. The $\chi^2$ analysis favors $J = 8$ as the most probable spin for the level. The reduced transition probabilities determined from the present lifetime and $\delta$ values ($\tau = 0.42^{+0.24}_{-0.14}$ ps and $\delta = 0.03 \pm 0.04$) support the earlier assignment of a positive parity to the 5824.3 keV level. The $B(E2)$ value calculated with $\delta = -9.51^{+3.43}_{-11.96}$, as reported by Berinde *et al.*,[9] is found to be too unrealistically enhanced.

*The 6452.4 keV level.* The 6452.4 keV level decays via the 1702.3 keV $\gamma$ transition. The present angular distribution measurements favor the assignment $J = 9$ for this level. This is in agreement with the result reported in Ref. 9. The possibility of $J = 7$ for this level, as suggested by Styczen *et al.*[8] is ruled out on the basis of the present angular distribution measurements. The two-point excitation function, reported by the same authors, however, also supports the assignment of $J = 9$.

The DSA measurements yield a meanlife of $\tau = 0.20^{+0.18}_{-0.12}$ ps for this level, which shows agreement within experimental errors with the only available earlier result[9] of $0.42^{+0.18}_{-0.15}$ ps. The value of meanlife for this level is corrected for the effects of cascade feedings from the two levels at 7237.1 and 8216.0 keV, the lifetimes for which were not known previously. Since these lifetimes have been measured in the present work, the effects of the cascade feedings have been appropriately accounted for. It is likely that the earlier result,[9] which apparently does not include this correction, is an overestimate.

The parity of the 6452.4 keV level was not known conclusively from the earlier measurements and was tentatively assigned to be positive. The present measurements also favor a positive parity assignment for this level, since it leads to a realistic $B(M1)$ value.

*The 6453.4 keV level.* The 6453.4 keV level decays via the 629.1 keV transition, consistent with the spin sequence $9_2^+ \rightarrow 8_2^+$, as found from the present angular distribution measurements. An upper limit of 2 ps is obtained for the meanlife of this level on the basis of an experimental $F(\tau) > 0.12$, observed at 55° to the beam direction. The angular distribution results lead to a mixing ratio $\delta = -0.22^{+0.08}_{-0.15}$ and hence, reduced transition probabilities $B(E2) > 7$ and $B(M1) > 0.06$ W.u. for the 629.1 keV transition. These results are consistent with the assignment of a positive parity to the 6453.4 keV state.

*The 7237.1 keV level.* This level decays via the 784.7 keV transition. No previous angular distribution results are available for the 784.7 keV $\gamma$ ray from the previous work of Berinde *et al.*[9] and Styczen *et al.*[8] due to a

strong interference caused by the intense 783 keV ($2^+ \rightarrow 0^+$) transition of $^{50}$Cr, as reported by the authors. The present experiment, which permits a reliable angular distribution measurement as there is no interference to the 784.7 keV transition, is consistent with a spin assignment of $J=10$ for the level and a multipole mixing ratio of $\delta=0.06^{+0.05}_{-0.03}$ for the depopulating transition. The DSA measurements at the three backward and one forward angles yield a meanlife of $\tau=0.23^{+0.22}_{-0.11}$ ps for the 7237.1 keV state. The lifetime value uncorrected for direct feeding effect is $0.24^{+0.21}_{-0.12}$ ps. No previous lifetime information is reported for the level.

The observed retardation factor for the predominant dipole component of the 784.7 keV transition favors the assignment of a positive parity to the 7237.1 keV state. This assignment is strengthened by the argument that the assumption of a negative parity leads to an unrealistic transition rate for the $E1$ component.

*The 8216.0 keV level.* The present angular distribution measurements on the 978.9 keV $\gamma$ ray depopulating the 8216.0 keV level show $J=11$ as the most probable spin for the level and $\delta=-0.10^{+0.08}_{-0.05}$ for the depopulating transition. A meanlife time of $\tau=0.35^{+0.25}_{-0.13}$ ps is obtained for the 8216.0 keV level using the DSA method. The sidefeeding time to the level is taken to be zero, since this is the highest energy level populated in the present work.

Assuming a positive parity for the 8216.0 keV state, the present lifetime and the mixing ratio values lead to the reduced transition probabilities $B(E2)=2.24^{+5.67}_{-2.19}$ W.u. and $B(M1)=0.10^{+0.05}_{-0.06}$ W.u. These results are consistent with a positive parity assignment. Assumption of a negative parity, on the other hand, leads to an unrealistic dipole transition rate. Hence a positive parity is assigned to the 8216.0 keV state.

### B. The nucleus $^{52}$Mn

The level scheme for $^{52}$Mn, obtained in the present work, is shown in Fig. 7. Excited states with energy up to 4163.4 keV and spin $J \leq 11$ have been populated. The five yrast levels at the energies 870.1, 2286.1, 2907.9, 3837.6, and 4163.4 keV are found to be preferentially populated via the reaction $^{51}$V($\alpha$,3n$\gamma$). Beside these, five lower spin states at 377.4, 732.0, 825.1, 1279.1, and 1683.4 keV have been populated comparatively weakly. The present $\gamma$-ray branching ratio for the 2037.8 and 621.8 keV transitions depopulating the 2907.9 keV state shows significant disagreement with the earlier result.[18] The branching ratio for the transitions from the 2286.1 keV state differs considerably with the value reported by Stefanini *el al.*[20] but agrees with that of Evers *et al.*[21].

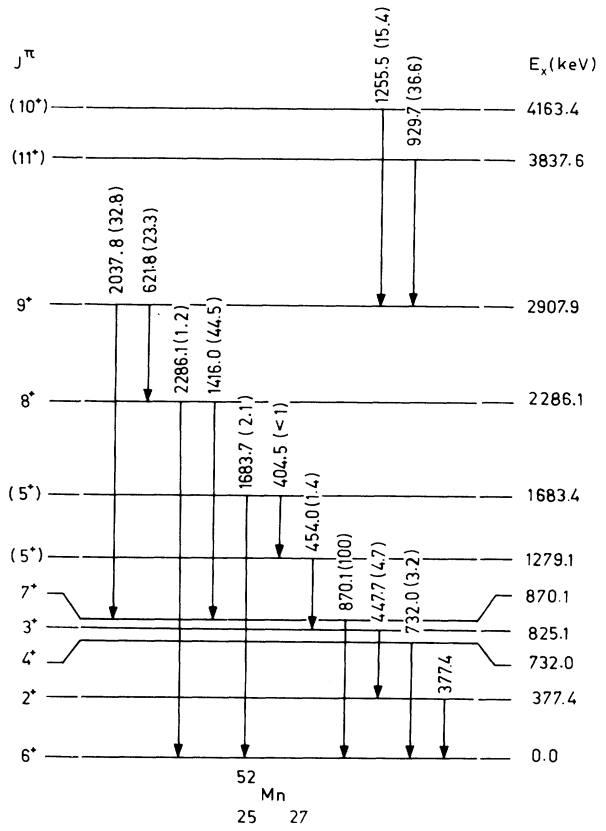


FIG. 7. Level scheme of $^{52}$Mn. The relative intensitites of the $\gamma$ rays observed in the reaction $^{51}$V($\alpha$,3n$\gamma$) $^{52}$Mn at 125° with respect to the beam direction and $E_\alpha=40$ MeV are given in parentheses. The errors in the relative intensity values are same as for $^{52}$Cr.

The placement of all the prominent $\gamma$-ray transitions in the level scheme, based on the three parameter coincidence relationships, is consistent with the earlier results.[18] As first reported by Evers *et al.*,[21] the 1255.5 keV transition is observed in coincidence with the 870.1 and 1416.0 keV energy windows but is not seen in coincidence with the energy gate at 929.7 keV. Hence it is reasonable to conclude that the 1255.5 keV transition connects the levels at 2907.9 and 4163.4 keV.

The results of the angular distribution measurements for the 621.8, 870.1, 929.7, and 1416.0 keV $\gamma$ rays are summarized in Table IV. The nature of the anisotropy in the angular distributions and the $\chi^2$ analyses show that the 621.8, 870.1, and 1416.0 keV transitions are

TABLE IV. Results of angular distribution measurements in $^{52}$Mn.

| Level energy $E_x$ (keV) | $\gamma$-ray energy $E_\gamma$ (keV) | Angular distribution coefficients $(A_2/A_0)_{exp}$ | $(A_4/A_0)_{exp}$ | Adopted spin sequence $J_i \rightarrow J_f$ | Multipole mixing ratio $\delta$ |
|---|---|---|---|---|---|
| 870.1 | 870.1 | −0.37±0.05 | −0.11±0.06 | 7→6 | $-0.04^{+0.03}_{-0.02}$ |
| 2286.1 | 1416.0 | −0.47±0.08 | 0.04±0.08 | 8→7 | $-0.13^{+0.03}_{-0.05}$ |
| 2907.9 | 621.8 | −0.25±0.08 | 0.01±0.09 | 9→8 | $-0.03^{+0.05}_{-0.03}$ |
| 3837.6 | 929.7 | 0.32±0.26 | −0.13±0.27 | 11→9 | $E2$ |

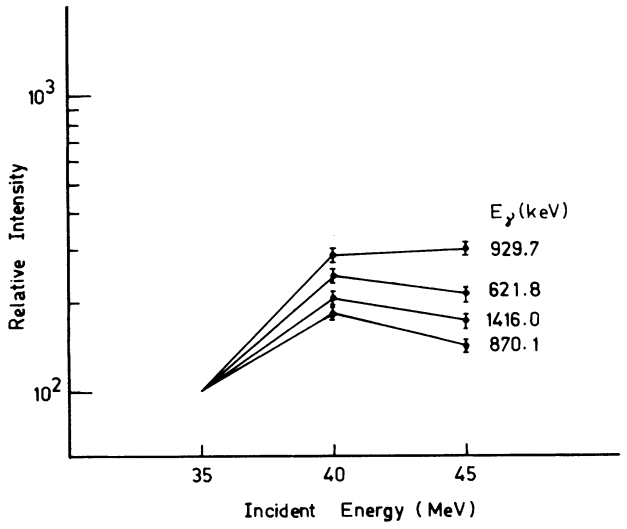


FIG. 8. Excitation functions for some prominent $\gamma$-ray transitions in $^{52}$Mn.

predominantly dipole in character. These, along with the results of the excitation function, shown in Fig. 8, are consistent with $J=7$, 8, and 9 for the levels at 870.1, 2286.1, and 2907.9 keV, as reported earlier.[18] However, the ambiguity regarding the spin of the 3837.6 keV level is not totally resolved. The present angular distribution results indicate that all the three spin values $J=9$, 10, and 11 are almost equally probable. Since the excitation function data (Fig. 8) do not favor $J=9$, the likely spin values for 3837.6 keV state are restricted to $J=10$ and 11. This is further discussed subsequently in the light of the lifetime results.

The spin assignment for the 4163.4 keV state could not be attempted since the 1255.5 keV $\gamma$ transition which depopulates this level undergoes large Doppler shifts and overlaps strongly with the 1251.5 keV line, belonging to $^{53}$Mn, at $\theta_\gamma=120°$ and 140°. The spin of the 4163.4 keV level is tentatively assigned $J=10$ on the basis of shell-model calculations, discussed in Sec. IV.

As stated earlier, the previous lifetime results, reported by Avrigeanu *et al.*,[10] measured by the DSA method, yielded only the upper limit values, mainly due to an interference from radioactive decay of a strongly excited $12^+$ isomeric state in $^{52}$Fe. This interference is absent in the present experiment since the reaction ($^{51}$V+$^4$He) does not permit the production of $^{52}$Fe. The present DSA measurements yield lifetime values for three levels at 870.1, 2907.9, and 4163.4 keV and an upper and a lower limit for the states at 2286.1 and 3837.6 keV, respectively. The lifetime of the 3837.6 keV state has been measured by the recoil distance method. The results of lifetime measurements, summarized in Table V, are discussed below for individual levels.

*The 870.1 keV level.* The mean lifetime of the 870.1 keV level is measured to be $\tau=0.07^{+0.08}_{-0.04}$ ps. The value is corrected for the effects of all observed cascade feedings as well as unobserved side feedings. The relatively large value of the upper limit of 0.55 ps, reported previously,[10] is attributed to the strong feeding effects mentioned earlier.

*The 2286.1 keV state.* The experimental attenuation factor for the 1416.0 keV transition which predominantly depopulates (branching ratio of ~97%) the 2286.1 keV state, is found to be $F(\tau)=0.54$ and corresponds to an uncorrected $\tau=0.28$ ps. Considering the effects of the long lived ($\tau=21.6\pm2.0$ ps) 3837.6 keV state which feeds the 2286.1 keV state via the $(11^+)\rightarrow9^+\rightarrow8^+$ cascade and assuming the sidefeeding time to the 2286.1 keV state to be zero, meanlife value of ~0.03 ps is obtained for this level. Since for a finite sidefeeding time, the result obtained is less than the above mentioned value, an upper limit of $\tau<0.1$ ps is assigned to the 2286.1 keV state. The corresponding lower limits of the $B(E2)$ values for the 1416.0 and 2286.1 keV transitions are consistent with the assignment of the spin and parity, $J^\pi=8^+$ for the level.

*The 2907.9 keV level.* This level decays via the 621.8 and the 2037.8 keV transitions with 41.6% and 58.4% branching, respectively. Since the 2037.8 keV $\gamma$-ray line

TABLE V. Results of lifetimes and reduced transition probabilities in $^{52}$Mn.

| $E_x$ (keV) | $E_\gamma$ (keV) $J_i^\pi\rightarrow J_f^\pi$ | Branching ratio (%) | Mixing ratio $\delta$ | Mean lifetimes $\tau$ (ps) Present | Previous | Reduced transition strength (W.u.) $E2$ | $M1$ |
|---|---|---|---|---|---|---|---|
| 870.1 | 870.1 $7^+\rightarrow6^+$ | 100 | $-0.04^{+0.03}_{-0.02}$ | $0.07^{+0.08}_{-0.04}$ | <0.55 | $3.3^{+13.8}_{-3.1}$ | $0.69^{+0.92}_{-0.37}$ |
| 2286.1 | 1416.0 $8^+\rightarrow7^+$ | 97.4 | $-0.13^{+0.03}_{-0.05}$ | <0.10 | <1.0 | >1.2 | >0.10 |
| | 2286.1 $8^+\rightarrow6^+$ | 2.6 | $E2$ | | | >0.34 | |
| 2907.9 | 621.8 $9^+\rightarrow8^+$ | 41.6 | $-0.03^{+0.05}_{-0.03}$ | 0.12±0.08 | <0.5 | $2.4^{+26.2}_{-1.8}$ | $0.46^{+0.91}_{-0.19}$ |
| | 2037.8 $9^+\rightarrow7^+$ | 58.4 | $E2$ | | | $9.9^{+19.7}_{-4.0}$ | |
| 3837.6 | 929.7 $(11^+)\rightarrow9^+$ | 100 | $E2$ | 21.6±2.0 | 21±1.5 | 4.74±0.50 | |
| 4163.4 | 1255.5 $(10^+)\rightarrow9^+$ | 100 | | $0.20^{+0.35}_{-0.16}$ | | | |

shows interference with an unassigned 2025 keV $\gamma$ ray due to large Doppler broadening in both, the experimental $F(\tau)$ is obtained from the centroid shift measurements on the 621.8 keV peak and the mean life of the level, corrected for feeding effects is determined to be $0.12\pm0.08$ ps. The $B(E2)$ and $B(M1)$ values for the 621.8 keV transition are $2.4^{+26.2}_{-1.8}$ W.u. and $0.46^{+0.91}_{-0.19}$ W.u., respectively, while the 2037.8 keV transition has a $B(E2)=9.9^{+19.7}_{-4.0}$ W.u. These results support the assignment of $J^{\pi}=9^{+}$ for the 2907.9 keV level.

*The 3837.6 keV level.* This level decays via the 929.7 keV transition to the $9^{+}$, 2907.9 keV state. The DSA measurements on the 929.7 keV $\gamma$-ray line yield only a lower limit of 5 ps for the mean life of the 3837.6 keV state.

The lifetime of the level was also measured by the recoil distance method. However, the measurement could not be carried out on the 929.7 keV line since the shifted component of the 935.6 keV line, due to the deexcitation of the 3114.4 keV state of $^{52}$Cr ($\tau=65$ ps) strongly interferes with the 929.7 keV peak. The 870.1 keV $\gamma$ transition which deexcites the 870.1 keV state in $^{52}$Mn was utilized for this purpose as it is expected to show the same decay characteristics as the 929.7 keV transition, the intermediate levels being all short lived ($\tau<1$ ps). The mean lifetime thus obtained is found to be $\tau=21.6\pm2.0$ ps, which is in excellent agreement with the previously reported value of $\tau=21.0\pm1.5$ ps. The effect of the direct population of the 870.1 keV level and the cascade feeding from the intermediate levels of interest was taken into account in the determination of the lifetime.

As outlined earlier, both $J=10$ and 11 are almost equally probable for the 3837.6 keV level and hence both $J$ values have been considered in the calculation of the reduced transition probabilities. The $E2$ transition rate is found to be enhanced with respect to the single particle estimate for both the possibilities, viz., $J^{\pi}=10^{+}$ and $11^{+}$. The 3837.6 keV state is tentatively assigned $J^{\pi}=11^{+}$ in view of the theoretical calculations which predict the $11^{+}$ state to lie below the $10^{+}$ state. As outlined earlier, the 4163.4 keV state is identified as the theoretically predicted $10^{+}$ state, lying above the $11^{+}$ state.

*The 4163.4 keV level.* The lifetime of the 4163.4 keV level is being reported for the first time. The 1255.5 keV transition which deexcites the 4163.4 keV level shows large Doppler broadening, signifying that the level has a short lifetime. The mean lifetime, determined from an analysis of the DSA data at the two forward angles 49° and 55°, is found to be $\tau=0.20^{+0.35}_{-0.16}$ ps.

## IV. DISCUSSION

The experimental results reported in Sec. III are discussed in the context of the available theoretical calculations below.

### A. The nucleus $^{52}$Cr

The properties of $^{52}$Cr have been extensively investigated in recent years in the framework of the shell model for (i) $^{52}$Cr has a magic number of $N=28$ neutrons and 4 protons in the $1f_{7/2}$ shell, and (ii) the high spin yrast states are expected to be rather pure in the shell-model sense and hence they can provide valuable information on the residual interactions in the $1f_{7/2}$ shell.

Excited states of $^{52}$Cr have been interpreted in the context of the shell-model calculations both in terms of pure and mixed configurations. Johnstone[4] performed calculations using specific $(p_{3/2}f_{5/2}p_{1/2})^{n_p}f_{7/2}^{-n_h}$ configurations relative to the $^{56}$Ni closed shell ($n_p$ and $n_h$ refer to the number of particles and holes, respectively), with the mass-independent effective interaction of Johnstone and Benson,[2] determined by least squares fits to empirical data. These calculations show that the ground state ($0^{+}$) and the states at 1434.0($2^{+}$), 2369.6($4_1^{+}$), 2767.6($4_2^{+}$) and 3114.4 keV($6_1^{+}$) predominantly belong to the 0p4h configuration. The 3614.7($5_1^{+}$) and 4750.1 keV($8_1^{+}$) levels also lie at excitation energies close to those predicted for 0p4h states. The close energy correspondence between the experimental and the theoretical levels makes it clear that the observed levels above 3.4 MeV, except the 3614.7 and 4750.1 keV states, are 1p5h states. The observed levels at 7237.1($10^{+}$) and 8216.0($11^{+}$) are predicted to lie at 7.3 and 8.1 MeV, respectively. The model also predicts yrast levels of spins 12, 13, and 14 at the energies 9.7, 10.35, and 12.35 MeV, respectively. These have not been observed experimentally so far. The observed levels have, however, been accounted for very well by these calculations and support the possibility that the eigenstates in $^{52}$Cr have a rather pure configurational structure.

A comparison of the observed electromagnetic transition rates with the calculations of Johnstone[4] shows that the calculated lifetime values are significantly larger than the measured ones for the levels at 3415.4($4_3^{+}$), 4015.8($5_2^{+}$) and 5824.3 keV($8_2^{+}$). The observed $\gamma$-ray branchings for many states above 3.4 MeV also show appreciable disagreement with these calculations. For example, the observed decay of the 3415.4 keV state predominantly to the 2767.6 keV level is not correctly reproduced in the calculations. However, as pointed out by Johnstone,[4] the discrepancies in the lifetime values and the $\gamma$-ray branchings may be accounted for by a weak ($<4\%$) mixing of the 0p4h component in the 1p5h configurations, assumed for these states.

Significantly, the new lifetime results reported in this work for the three high spin states at 6453.4($9_2^{+}$), 7237.1($10^{+}$) and 8216.0($11^{+}$) show close agreement with the calculated ones (Table VI). The experimentally measured multipole mixing ratio $\delta=0.06^{+0.05}_{-0.03}$, reported in this work for the 784.7 keV $10^{+}\rightarrow9_1^{+}$ transition depopulating the 7237.1 keV state, is in excellent agreement with the calculated value of $\delta=0.06$. The fair overall agreement of these calculations[4] with the experimental level scheme and the observed electromagnetic properties in $^{52}$Cr lends support to the assumption that the high spin states in $^{52}$Cr have almost pure 1p5h configuration and only weak configuration mixing is required to account for the observed properties.

The calculations of Styczen *et al.*,[8] performed in a

TABLE VI. Comparison of experimental and theoretical (Ref. 4) results on $\gamma$-ray branching ratios, level lifetimes, and multipole mixing ratios for high spin states in $^{52}$Cr. The experimental results are from the present work unless indicated otherwise.

| $E_x$ (keV) | $E_\gamma$ (keV) $J_i^\pi \rightarrow J_f^\pi$ | Branching ratio (%) Expt. | Theor. | Level lifetimes (ps) Expt. | Theor. | Multipole mixing ratio $\delta$ Expt. | Theor. |
|---|---|---|---|---|---|---|---|
| 6453.4 | 629.1 $9^+ \rightarrow 8^+$ | 100<br>26[a]<br>100[b] | 62[c] | $<2.0$ | 2.4[c] | $-0.22^{+0.08}_{-0.15}$<br>$0.14\pm0.06$[a] | 0.21[c] |
| 7237.1 | 784.7 $10^+ \rightarrow 9^+$ | 100<br>100[a,b] | 96 | $0.23^{+0.22}_{-0.11}$ | 0.13 | $0.06^{+0.05}_{-0.03}$ | 0.06 |
| 8216.0 | 978.9 $11^+ \rightarrow 10^+$ | 100<br>100[a,b] | 73 | $0.35^{+0.25}_{-0.13}$ | 0.19 | $-0.10^{+0.08}_{-0.05}$ | 0.13 |

[a]Reference 8.
[b]Reference 9.
[c]Results for the theoretically predicted $9^+$ level at $\sim 6.4$ MeV.

model space which includes $(f_{7/2})^n$ and $[(f_{7/2})^{n-1}j]$ configurations with $A=40+n$, where $j=2p_{3/2}$, $2p_{1/2}$, or $1f_{5/2}$, show that the observed levels not belonging to the $(f_{7/2})^n$ family result due to a single neutron excitation into the $2p_{3/2}$ shell with at most 10% admixture of the $1f_{5/2}$ excitation. The mixing between the two types of configurations, viz., $(f_{7/2})^n$ and $[(f_{7/2})^{n-1}; (2p_{3/2}, 2p_{1/2}, 1f_{5/2})]$ is found to be very small, with not more than 1% $(f_{7/2})^n$ admixture in these states. As predicted by these calculations, the in-band transitions between the high-spin states not belonging to the $(f_{7/2})^n$ configuration, are experimentally observed to be predominantly $M1$ in nature with small multipole mixing ratios.

However, the lower lying levels have been shown in the calculations of Styczen *et al.*[8] to contain about 80% of the $(f_{7/2})^n$ configuration, rather than being pure $(f_{7/2})^n$, as reported by Johnstone.[4] Clearly, the 20% admixture involving a neutron excitation to the $2p_{3/2}$ and $1f_{5/2}$ shells and to a smaller extent, proton excitation, is sufficient to bring the calculated results in closer agreement with the experiment.

### B. The nucleus $^{52}$Mn

For $^{52}$Mn, van Hees and Glaudemans[5] performed shell-model calculations both in the simple $f^n_{7/2}$ and $f^n_{7/2}+[(f^{n-1}_{7/2}),p_{3/2}f_{5/2}p_{1/2}]$ extended model space, where $n$ denotes the number of active particles outside the $^{40}$Ca core. Though the predicted levels in both the model spaces generally agree within 200 keV with the observed levels, the mean deviation from the latter is 116 keV for the simple $f^n_{7/2}$ model in contrast to 85 keV for the enlarged model space. All the observed levels have a predominantly $f^n_{7/2}$ character. The spins for all the levels with $J \leq 11$ are reproduced in these calculations. The observed level at 4163.4 keV is identified as the $J=10$ state predicted by theory. The predicted excitation energy of the $J=10$ state is, however, found to deviate by $\sim 275$ keV from the observed value in both the calculations.

A comparison of the present experimental electromagnetic transition probabilities with the theoretical calculations of van Hees and Glaudemans,[5] presented in Table VII, shows that for both $M1$ and $E2$ transitions, there is a fair agreement between the observed and the predicted results in the simple $f^n_{7/2}$ as well as the extended model spaces.

Mooy and Glaudemans[7] performed shell model calculations in the configuration space specified by $f^{-n}r^m+f^{-n-1}r^{m+1}$ where $f$ denotes the $1f_{7/2}$ orbit and $r$ stands for any of the other $fp$-shell orbits, $2p_{3/2}$, $2p_{1/2}$, and/or $1f_{5/2}$. The numbers $n$ and $m$, defined with respect to the doubly magic $^{56}$Ni core, represent the minimum number of holes and particles, respectively, needed to describe the ground state of the nucleus. The calculated spectrum for $^{52}$Mn shows that the $J=10$ state is again predicted to have a higher excitation energy than the $J=11$ state. Also the excitation energy of these two states agree well with the observed values. The correspondence between the excitation energies of the model calculations with experiment is also found to be remarkably good.

TABLE VII. Comparison of the experimental and theoretical transition rates for $M1$ and $E2$ transitions between predominantly $f^n_{7/2}$ states in $^{52}$Mn.

| $J_i^\pi \rightarrow J_f^\pi$ | Strength of $M1$ transitions (W.u.) Theory (model space)[a] ($f^n$) | $f^n+f^{n-1}r$ | Experiment (present) | Strength of $E2$ transitions (W.u.) Theory (model space)[a] ($f^n$) | $f^n+f^{n-1}r$ | Experiment (present) |
|---|---|---|---|---|---|---|
| $7^+ \rightarrow 6^+$ | 0.68 | 0.36 | $0.69^{+0.92}_{-0.37}$ | 4.7 | 9.0 | $3.25^{+13.8}_{-3.1}$ |
| $8^+ \rightarrow 7^+$ | 0.40 | 0.32 | $>0.10$ | | | $>1.20$ |
| $8^+ \rightarrow 6^+$ | | | | 1.9 | 2.5 | $>0.34$ |
| $9^+ \rightarrow 8^+$ | 1.04 | 0.45 | $0.46^{+0.91}_{-0.19}$ | | | $2.4^{+26.2}_{-1.8}$ |
| $9^+ \rightarrow 7^+$ | | | | 4.1 | 5.0 | $9.87^{+19.7}_{-4.0}$ |
| $11^+ \rightarrow 9^+$ | | | | 3.6 | 4.7 | $4.74\pm0.50$ |

[a]Reference 5.

Mooy and Glaudemans[7] also showed that two microscopically calculated bands with $K=3$ and $K=6$ exist in $^{52}$Mn, the observables of which could be described well by an axially symmetric rotor model. The $3_1^+, 4_2^+, 5_2^+$, and $6_3^+$ states are identified as members of the $K=3$ band, and $6_1^+$ (g.s.), $7_1^+$, and $8_1^+$ states as the members belonging to the $K=6$ band in $^{52}$Mn. The experimental $M1$ and $E2$ transition rates for the $8_1^+ \rightarrow 7_1^+$ and $7_1^+ \rightarrow 6_1^+$ transitions in the present work agree within their error limits with the rotational model values. The ratio $B/A$ which determines the deviations from the $J(J+1)$ dependence of the excitation energies, characteristic of rotational bands, is found to be $\sim 10^{-2}$ for $^{52}$Mn, as for most $fp$-shell nuclei which display rotational properties. This shows that $^{52}$Mn, like many of the $fp$-shell nuclei, can be considered to be a softer rotor compared to the nuclei in the rare-earth region, where $B/A \sim 10^{-3}$.

## ACKNOWLEDGMENTS

The authors thank the operating staff of the Cyclotron for the running of the machine and the staff of the Norsk Data Computer system for their cooperation. They are grateful to R. K. Bhowmik, R. P. Sharma, and S. K. Basu for help during experiments, S. K. Pardha Saradhi for preparation of targets and S. N. Chintalapudi for his co-operation. Thanks are due to Professor P. N. Mukherjee for his comments and A. K. Mitra, A. K. Kindu, D. Banik, R. Ghosh, and D. C. Ghosal for their technical assistance.

[1]K. Lips and M. T. McEllistrem, Phys. Rev. C **1**, 1009 (1970).
[2]I. P. Johnstone and H. G. Benson, J. Phys. G **3**, L69 (1977).
[3]A. Yokoyama, T. Oda, and H. Horie, Prog. Theor. Phys. **60**, 427 (1978).
[4]I. P. Johnstone, Phys. Rev. C **17**, 1428 (1978).
[5]A. G. M. van Hees and P. W. M. Glaudemans, Z. Phys. A **303**, 267 (1981).
[6]W. Kutschera, B. A. Brown, and K. Ogawa, Rivista Nuovo Cimento **1**, 1 (1978).
[7]R. B. M. Mooy and P. W. M. Glaudemans, Z. Phys. A **312**, 59 (1983).
[8]J. Styczen, E. Bozek, T. Pawlat, Zb. Stachura, E. A. Beck, C. Gehringer, B. Haas, J. C. Merdinger, N. Schulz, P. Taras, M. Toulemonde, J. P. Vivien, and A. Muller-Arnke, Nucl. Phys. **A327**, 295 (1979).
[9]A. Berinde, R. O. Dumitru, N. Grecescu, I. Neamu, C. Protop, N. Scintei, C. M. Simonescu, B. Heits, H. W. Schuh, P. von Brentanu, and K. O. Zell, Nucl. Phys. **A284**, 65 (1977).
[10]V. Avrigeanu, D. Bucurescu, G. Constantinescu, E. Dragulescu, M. Ivascu, D. Pantelica, and R. Teodorescu, Nucl. Phys. **A272**, 243 (1976).
[11]H. Ejiri, T. Shibata, A. Shimizu and K. Yogi, J. Phys. Soc. Jpn. **33**, 1515 (1972).
[12]E. Der Mateosian and A. W. Sunyar, At. Data Nucl. Data Tables **13**, 391 (1974).
[13]E. K. Warburton, J. W. Olness, and A. R. Poletti, Phys. Rev. **160**, 938 (1967).
[14]P. Banerjee, B. Sethi, J. M. Chatterjee, P. Bhattacharya, and A. K. Sengupta, Il Nuovo Cimento **85A**, 54 (1985).
[15]T. K. Alexander and A. Bell, Nucl. Instrum. Methods **81**, 22 (1970).
[16]P. Banerjee, B. Sethi, J. M. Chatterje, and R. K. Chattopadhyay, Nucl. Instrum. Methods **202**, 431 (1982).
[17]A. R. Poletti, B. A. Brown, D. B. Fossan, and E. K. Warburton, Phys. Rev. C **10**, 2329 (1974).
[18]J. R. Beene, Nucl. Data Sheets **25**, 235 (1978).
[19]S. W. Sprague, R. G. Arns, B. J. Brunner, S. E. Caldwell, and C. M. Rosza, Phys. Rev. C **4**, 2074 (1971).
[20]A. M. Stefanini, C. Signorini, M. Morando and R. A. Ricci, Nuovo Cimento **33A**, 460 (1976).
[21]D. Evers, A. Harasim, R. L. McGrath, and W. Assmann, Phys. Rev. C **15**, 1690 (1977).
[22]C. F. Monahan, N. Lawley, C. W. Lewis, I. G. Main, M. F. Thomas, and P. J. Twin, Nucl. Phys. **A120**, 460 (1968).
[23]N. Bendjaballah, B. Delaunay, J. Delaunay, and T. Nomura, Nucl. Phys. **A280**, 228 (1977).